Huang, J., Huang, J.-X., Griffin, W.L., and Huang, F., 2022, Zn-, Mg- and O-isotope evidence for the origin of mantle eclogites from Roberts Victor kimberlite (Kaapvaal Craton, South Africa): Geology, https://doi.org/10.1130/G49780.1

Supplemental Material

Zn-, Mg- and O-isotope evidence for the origin of mantle eclogites from Roberts Victor kimberlite (Kaapvaal Craton, South Africa)

Jian Huang[1,2*], Jin-Xiang Huang[3], William L. Griffin[3], Fang Huang[1,2]

[1]*Chinese Academy of Sciences Key Laboratory of Crust-Mantle Materials and Environments, School of Earth and Space Sciences, University of Science and Technology of China, Hefei 230026, China*

[2]*Chinese Academy of Sciences Center for Excellence in Comparative Planetology*, *University of Science and Technology of China, Hefei 230026, China*

[3]*Australian Research Council Centre of Excellence for Core to Crust fluid Systems, Department of Earth and Environmental Sciences, Macquarie University, NSW 2109, Australia*

*E-mail: jianhuang@ustc.edu.cn

1. Analytical methods

1.1. Zinc contents

Zinc contents of garnet (gnt), clinopyroxene (cpx) and whole rocks for most eclogite samples have been reported previously by Huang et al. (2012). We here only determine the Zn contents of gnt and cpx with no data reported in Huang et al. (2012). Optically clean gnt grains from samples RV07-1, -07, -08, -16, -18 and -19 as well as optically clean gnt and cpx grains from samples HRV?, 344 and 345a were handpicked under binocular microscope, mounted in epoxy resin and polished down to expose grain centers. The mounted gnt and cpx grains were analyzed by LA-ICPMS at the University of Science and Technology of China (USTC) using the methods described by Liu et al. (2008). Three gnt or cpx grains from individual eclogite samples were analyzed by LA-ICPMS and the average Zn contents of the results of three measurements were used in this study (Table S1).

1.2. Magnesium isotopes

Magnesium isotope measurements were conducted at the USTC using the established procedures by An et al. (2014). In this study, we only determined the Mg-isotope compositions of cpx separates from eclogites RV07-30, -31, -33 and -34, because gnt separates from these four eclogites as well as cpx and gnt separates from other eclogites investigated here had been determined for the Mg-isotope compositions in a previous study (Huang et al., 2016a). Optically clean cpx grains were first handpicked under binocular microscope and then cleaned three times with ethanol in an ultra-sonic bath for 10 minutes,

followed by dissolving them in 7 ml capped Savillex beakers using double-distilled concentrated HF + HNO_3, HCl + HNO_3 and HNO_3 successively. After full dissolution and evaporation of acid, the final nitrates were dissolved in 1 ml 2N HNO_3 for chromatographic purification of Mg. Magnesium was separated using 2 ml pre-cleaned Bio-Rad cation resin (AG50-X12) conditioned with 2 N HNO_3. Matrix elements were removed using 2 N HNO_3 + 0.5N HF and Mg was eluted using 1 N HNO_3. The column chemistry was performed twice to efficiently purify Mg from matrix elements and obtain a pure Mg solution. The Mg yields were assessed by analyzing Mg contents in the elution collected before and after the Mg cut. The Mg yields through column chemistry are better than 99.5% and the total procedural blank (from sample dissolution to mass spectrometry) of Mg 9.9 ng, negligible compared to ≥20 μg Mg loaded on the resin.

A sample-standard bracketing method was applied to correct instrumental mass bias and time drifts. Magnesium solutions were diluted to 0.5 ppm in 2% HNO_3 and bracketed with DSM-3 at the same concentration. Three Mg isotopes (^{24}Mg, ^{25}Mg, and ^{26}Mg) were measured in static mode on L3, C, and H3 Faraday cups, respectively. A Ni(H) + Ni (Jet) cone assembly was used with the ^{24}Mg sensitivity of ~30 V/ppm under low mass resolution conditions (M/ΔM of ~400). Magnesium-isotope ratios are reported in standard δ-notation in per mil relative to Mg standard DSM-3: $\delta^{X}Mg = [(^{X}Mg/^{24}Mg)_{sample}/(^{X}Mg/^{24}Mg)_{DSM\text{-}3} - 1] \times 1000‰$, where X = 25 or 26. The $\delta^{26}Mg$ of USGS standard BIR-1 processed together with cpx separates is −0.19 ± 0.02‰, in good agreement with those of previous studies (An and Huang, 2014; Teng, 2017 and references therein). The Mg-isotope results were listed in Table S1.

1.3. Zinc isotopes

Zinc isotope measurements were carried out at the USTC using the procedures established by Chen et al. (2016) and Yang et al. (2018). Optically clean mineral grains (i.e., gnt and cpx) were first handpicked under binocular microscope and then cleaned three times with ethanol in an ultrasonic bath for 10 minutes. Depending on the Zn contents of whole rocks, gnt and cpx, whole-rock powders (~16 – 49 mg) and mineral separates (~12 – 27 mg) were dissolved in 7 ml capped Savillex beakers using double-distilled concentrated HF + HNO_3, HCl + HNO_3 and HCl successively. After complete digestion and evaporation of the acid solution, the final chlorides were dissolved in 1 ml 6 N HCl to provide a stock bulk solution ready for chromatographic purification of Zn. Zinc was efficiently purified by 2 ml (first step) and 0.5 ml (second step) of pre-cleaned Bio-Rad AG-MP-1M strong anion exchange resin in a 0.5N HNO_3 media. The purified Zn was finally dissolved in 2% HNO_3 prior to MC-ICPMS analysis. The Zn yields, based on analyses of Zn contents in the elution collected before and after the Zn cut, are >99%. The total procedural blanks range from 4.1 to 4.8 ng, and are negligible compared to ~1.2 − 2.0 μg Zn loaded onto the resin.

Zinc-isotope ratios were measured using a Thermo-Fisher *Neptune Plus* MC-ICPMS at

the USTC. The ^{70}Zn-^{67}Zn double-spike method was applied to correct instrumental mass bias and time drifts (Yang et al., 2018). The double-spike solution has a Zn concentration of 2.67 ppm, a $^{70}Zn/^{67}Zn$ ratio = 1.02, and a ratio of (^{70}Zn + ^{67}Zn) to total Zn = ~0.45, yielding molar ratios of about 1 : 0.6 : 0.8 : 0.5 : 0.8 for ^{64}Zn : ^{66}Zn : ^{67}Zn : ^{68}Zn : ^{70}Zn in the spike-sample mixture. The double-spike solution was added to the purified Zn solution after column chemistry, and the Zn concentration of the spike-sample mixture was 300 ppb in 2% HNO_3. Five Zn isotopes (64, 66, 67, 68, and 70) were simultaneously collected by L3, L1, C, H1, and H3 Faraday cups, respectively. A Ni (H) + Ni (Jet) cone assembly was used with the ^{64}Zn sensitivity of ~18 V/ppm.

The NIST SRM 683 standard was used as an in-house "zero-delta" reference material during the course of this study. Zinc-isotope ratios are expressed/processed as $\delta^{X}Zn_{sample\text{-}SRM683} = [(^{X}Zn/^{64}Zn)_{sample}/(^{X}Zn/^{64}Zn)_{SRM\ 683} - 1] \times 1000‰$, where X = 66, 67, 68, or 70. To facilitate the comparison of our data with previously-published data normalized to the international reference material JMC Lyon Zn standard 3-0749L, the $\delta^{X}Zn_{sample\text{-}JMC}$ values (= $\delta^{X}Zn_{sample\text{-}SRM683}$ + 0.12‰, Chen et al., 2016; Yang et al., 2018) were used in this study. Two in-house pure Zn standards (IRMM3702 and AAS) were regularly analyzed to monitor instrumental stability and data reproducibility during the course of this study. Repeated analyses of IRMM3702 and AAS yielded $\delta^{66}Zn$ = 0.27 ± 0.03‰ (2SD, n = 38) and 0.04 ± 0.03‰ (2SD, n = 38), respectively. The measured $\delta^{66}Zn$ values of USGS standards processed with the investigated eclogites and minerals separates are 0.32 ± 0.04‰ (2SD, n = 8) for BHVO-2 and 0.20 ± 0.04‰ (2SD, n = 6) for BIR-1 (Table S1). These values agree well within error with previously published values (Chen et al., 2013, 2016; Sossi et al., 2015; Doucet et al., 2016; Huang et al., 2016, 2018a, b; Moynier et al., 2017; Wang et al., 2017). This, combined with consistent results for repeated analyses (Table S1), assures the accuracy and precision of our Zn isotopic data.

2. Modelling the Zn-Mg isotope covariation caused by diffusional fractionation

High temperature diffusion driven by gradients of chemical activity and associated kinetic isotope fractionation mainly depend on three variables: (1) the diffusion coefficients of the element (D), (2) gradients of element concentrations between two phases, and (3) the kinetic isotope fractionation parameter (β) (Richter et al., 2009). The isotope diffusion coefficients and β are related by the equation:

$$D_1/D_2 = (m_2/m_1)^{\beta} \quad \text{..... (1)}$$

In equation (1), D_1 and D_2 are the diffusion coefficients of isotopes with the masses m_1 and m_2 (Richter et al., 2009).

In this study, chemical diffusion-driven isotope fractionation occurred between MORB-like melts and peridotites during the migration of melts along conduits in the asthenosphere.

The lower Zn and higher MgO contents in peridotites relative to melts facilitate the preferential diffusion of ^{64}Zn from melts to peridotites and of ^{24}Mg from peridotites to melts during melt-peridotite reaction, as diffusion occurs along gradients of chemical activity and light isotopes diffuse faster than heavy ones (Richter et al., 2009). For modelling the covariation of Zn-Mg-isotope ratios of melts caused by diffusional fractionation between melts and peridotites, we here assume that melts have a spherical shape, and starting Mg-Zn elemental contents and isotopic compositions equal to MORB (Table S3). Considering that the asthenosphere mantle predominantly consist of peridotites and that deep-seated melts are small in volume, the ambient peridotites can be taken as an effectively infinite reservoir with Mg-Zn elemental contents and isotopic compositions equal to fertile mantle (or primitive mantle) (Table S3).

The following equations (2)-(5), combined with equation 1, are used to model the covariations of Zn-Mg-isotope ratios caused by diffusional fractionation.

Elemental and isotopic concentrations satisfy Fick's diffusion equation (Crank, 1975):

$$\frac{\partial C}{\partial t} = \frac{D}{r^2}\frac{\partial}{\partial r}\left(r^2\frac{\partial C}{\partial r}\right) \quad \text{(2)}$$

With initial condition $C\big|_{t=0} = C_0$ and boundary condition $C\big|_{r=a} = C_1$, we can get the equation (3):

$$C = C_1 + (C_1 - C_0)\frac{2a}{\pi r}\sum_{n=1}^{\infty}\frac{(-1)^n}{n}\sin\frac{n\pi r}{a}e^{-Dn^2\pi^2 t/a^2} \quad \text{(3)}$$

The concentrations in centre of sphere (r = 0) can be obtained by equation (4):

$$C = C_1 + 2(C_1 - C_0)\sum_{n=1}^{\infty}(-1)^n e^{-Dn^2\pi^2 t/a^2} \quad \text{(4)}$$

Assuming the concentrations of the centre of sphere represent those of the melts, the isotopic compositions can be expressed as:

$$\delta = \left(\frac{C_a}{C_b} - 1\right)\times 1000‰ \quad \text{(5)}$$

Using the parameters listed in Table S3 and setting the radius of basaltic melt sphere as 1m, we can obtain the covariations of Zn-Mg-isotope ratios caused by diffusional fractionation. The Zn-Mg-isotope ratios of Type II eclogites from Roberts Victor can best be reproduced at D_{Zn}/D_{Mg} = 1 to 2 (Fig. 2d).

Table S1. Zn-Mg-O isotope compositions and Zn contents of reference materials, whole rocks, garnet and cpx of the Roberts Victor eclogites.

Sample	Type	Rock[a] /Mineral	Mode[a] (%)	Zn_{Rec} /Zn[b](ppm)	$\delta^{66}Zn$[c] (‰)	2SD[d]	$\delta^{68}Zn$[c] (‰)	2SD[d]	N[e]	$\delta^{25}Mg$[c] (‰)	2SDd	$\delta^{26}Mg$[c] .(‰)	2SD[d]	N[e]	$\delta^{66}Zn_{Rec}$[f] (‰)	2sd[g]	$\delta^{26}Mg_{Rec}$[f] (‰)	2sd[g]	$\delta^{18}O_{garnet}$[h] (‰)
RV07-02	I	WR		73.0	0.30	0.00	0.59	0.01	2						0.31	0.04	-0.2	0.07	
		garnet	27.5	84.4	0.22	0.01	0.45	0.00	2	-0.27	0.03	-0.52	0.05	15					6.84
		Cpx	72.5	68.7	0.35	0.02	0.74	0.05	2	0.01	0.02	0.01	0.04	9					
RV07-03	I	WR		57.9	0.25	0.02	0.51	0.01	2						0.28	0.04	-0.61	0.07	
		garnet	62.3	60.2	0.27	0.01	0.51	0.07	2	-0.38	0.06	-0.74	0.09	9					6.04
		Cpx	37.7	53.9	0.29	0.05	0.57	0.06	2	-0.15	0.02	-0.29	0.04	9					
RV07-09a	I	WR		59.5	0.49	0.01	0.96	0.03	2						0.43	0.04	-0.4	0.07	
		Replicate[i]			0.50	0.02	0.99	0.05	2										
		garnet	25.3	91.4	0.27	0.01	0.55	0.00	2	-0.36	0.02	-0.70	0.05	9					8.52
		Cpx	52.5	69.4	0.52	0.02	1.03	0.03	2	-0.05	0.02	-0.10	0.02	8					
RV07-09b	I	WR		89.9	0.33	0.01	0.65	0.03	2										
RV07-13	I	WR		82.3	0.25	0.01	0.49	0.03	2						0.32	0.04	-0.47	0.07	
		garnet	42.0	98.9	0.40	0.03	0.81	0.06	2	-0.41	0.06	-0.79	0.09	3					7.98
		Replicate[i]			0.37	0.00	0.73	0.01	2										
		Cpx	58.0	70.2	0.24	0.00	0.47	0.01	2	-0.07	0.01	-0.16	0.02	3					
		Replicate[i]			0.21	0.01	0.40	0.01	2										
RV07-20	I	WR		42.7	0.06	0.01	0.12	0.03	2						0.03	0.04	-0.39	0.07	
		garnet	54.6	44.5	0.01	0.00	0.01	0.03	2	-0.30	0.01	-0.58	0.03	6					6.53
		Cpx	45.4	40.6	0.07	0.03	0.14	0.02	2	-0.03	0.02	-0.08	0.03	3					
RVF-6	I	WR		139.9											0.35	0.04	-0.57	0.07	
		garnet	50.0	138.6	0.30	0.01	0.58	0.00	2	-0.43	0.02	-0.85	0.06	6					9.08
		Cpx	50.0	141.2	0.40	0.01	0.77	0.00	2	-0.15	0.01	-0.30	0.02	3					

Continued next page

Sample	Type	Rock[a] /Mineral	Mode[a] (%)	Zn_{Rec} /Zn[b](ppm)	$\delta^{66}Zn$[c](‰)	2SD[d]	$\delta^{68}Zn$[c] (‰)	2SD[d]	N[e]	$\delta^{25}Mg$[c] (‰)	2SD[d]	$\delta^{26}Mg$[c] (‰)	2SD[d]	N[e]	$\delta^{66}Zn_{Rec}$[f]	2sd[g]	$\delta^{26}Mg_{Rec}$[f]	2sd[g]	$\delta^{18}O_{garnet}$[h] (‰)
RV07-01	I	WR		46.9	0.25	0.02	0.50	0.06	2						0.25	0.04	-0.3	0.07	
		garnet	41.8	***55.9***	0.22	0.02	0.43	0.02	2	-0.27	0.04	-0.53	0.03	6					6.69
		Replicate[i]			0.20	0.02	0.40	0.01	2										
		Cpx	58.2	40.4	0.28	0.02	0.56	0.03	2	-0.01	0.01	-0.02	0.02	6					
		Replicate[i]			0.30	0.00	0.59	0.03	2										
RV07-07	I	WR		***59.6***	0.26	0.01	0.50	0.05	2						0.24	0.04	-0.4	0.07	
		garnet	55.0	***68.3***	0.22	0.02	0.45	0.01	2	-0.29	0.03	-0.56	0.07	6					6.65
		Cpx	45.0	48.9	0.27	0.00	0.53	0.02	2	-0.03	0.02	-0.08	0.04	6					
RV07-11	I	WR		68.2	0.25	0.01	0.48	0.00	2						0.25	0.04	-0.6	0.07	
		garnet	53.3	80.8	0.23	0.01	0.46	0.04	2	-0.40	0.02	-0.77	0.04	6					6.53
		Cpx	46.7	53.8	0.28	0.01	0.54	0.02	2	-0.14	0.03	-0.29	0.05	9					
RV07-14	I	WR		67.5	0.22	0.00	0.42	0.02	2						0.22	0.04	-0.46	0.07	
		garnet	70.3	75.4	0.22	0.02	0.45	0.03	2	-0.29	0.04	-0.56	0.05	5					6.23
		Cpx	29.7	48.7	0.21	0.01	0.43	0.06	2	-0.03	0.03	-0.06	0.04	12					
RV07-16	I	WR		***80.3***	0.20	0.00	0.40	0.02	2						0.2	0.04	-0.5	0.07	
		Grt	58.3	***92.8***	0.19	0.01	0.36	0.08	2	-0.32	0.02	-0.62	0.04	12					6.25
		Cpx	41.7	62.8	0.23	0.01	0.45	0.01	2	-0.07	0.03	-0.16	0.06	9					
RV07-18	I	WR		63.6	0.26	0.03	0.48	0.00	2						0.25	0.04	-0.31	0.07	
		garnet	67.0	72.0	0.24	0.03	0.49	0.08	2	-0.19	0.02	-0.38	0.03	6					6.14
		Cpx	33.0	46.6	0.27	0.00	0.54	0.00	2	-0.02	0.04	-0.04	0.06	15					
RV07-19	I	WR		***56.4***	0.24	0.04	0.48	0.07	2						0.26	0.04	-0.4	0.07	
		garnet	67.9	***65.0***	0.26	0.05	0.50	0.07	2	-0.26	0.03	-0.50	0.05	12					6.17
		Cpx	32.1	38.3	0.29	0.02	0.58	0.02	2	0.02	0.04	0.03	0.06	14					

Continued next page

Sample	Type	Rock[a] /Mineral	Mode[a] (%)	Zn_{Rec} /Zn[b](ppm)	$\delta^{66}Zn$[c] (‰)	2SD[d]	$\delta^{68}Zn$[c] (‰)	2SD[d]	N[e]	$\delta^{25}Mg$[c] (‰)	2SDd	$\delta^{26}Mg$[c] (‰)	2SD[d]	N[e]	$\delta^{66}Zn_{Rec}$[f] (‰)	2sd[g]	$\delta^{26}Mg_{Rec}$[f] (‰)	2sd[g]	$\delta^{18}O_{garnet}$[h] (‰)
RV07-12	II	WR		102.9	0.44	0.04	0.88	0.00	2								-0.46	0.07	
		Replicate[i]			0.45	0.00	0.97	0.00	2						0.42	0.04			
		garnet	48.3	100.3	0.39	0.01	0.78	0.01	2	-0.34	0.03	-0.66	0.02	12					3.04
		Cpx	51.7	103.4	0.45	0.01	0.91	0.01	2	-0.15	0.04	-0.30	0.04	9					
RV73-12	II	WR		108.0	0.34	0.04	0.71	0.07	2						0.38	0.04	-0.17	0.07	3.52
		garnet	45.3	128.2	0.38	0.04	0.76	0.02	2	-0.20	0.02	-0.36	0.03	12					
		Cpx	54.7	91.5	0.39	0.05	0.78	0.06	2	0.12	0.03	0.22	0.06	9					
HRV-?	II	WR		***64.7***											0.46	0.04	-1.01	0.07	
		garnet	50.0	***71.0***	0.43	0.02	0.83	0.02	2	-0.65	0.04	-1.26	0.07	8					4.88
		Cpx	50.0	***58.4***	0.50	0.00	0.99	0.01	2	-0.37	0.03	-0.73	0.03	6					
HRV344	II	WR		***62.0***											0.48	0.04	-1.09	0.07	
		garnet	50.0	***63.8***	0.44	0.01	0.89	0.06	2	-0.73	0.04	-1.41	0.03	6					4.80
		Cpx	50.0	***60.3***	0.53	0.02	1.03	0.02	2	-0.37	0.02	-0.72	0.03	6					
HRV345	II	WR		***65.4***											0.54	0.04	-1.06	0.07	
		garnet	50.0	***64.7***	0.50	0.02	0.98	0.05	2	-0.69	0.04	-1.35	0.06	9					4.74
		Cpx	50.0	***66.1***	0.58	0.02	1.16	0.03	2	-0.37	0.03	-0.73	0.02	6					
RV07-08	II	WR		***67.0***	0.22	0.03	0.46	0.06	2						0.24	0.04	-0.37	0.07	
		garnet	40.1	***65.0***	0.14	0.01	0.28	0.02	2	-0.36	0.03	-0.70	0.05	15					2.91
		Cpx	59.9	77.4	0.30	0.01	0.58	0.03	2	-0.05	0.03	-0.09	0.03	12					
RV07-30	II	WR		89.7											0.30	0.04	-0.14	0.07	
		garnet	50.0	105.9	0.27	0.03	0.53	0.04	2	-0.26	0.01	-0.49	0.04	3					2.5
		Cpx	50.0	73.6	0.35	0.05	0.67	0.01	2	***0.11***	***0.01***	***0.21***	***0.02***	***3***					

Continued next page

Sample	Type	Rock[a] /Mineral	Mode[a] (%)	Zn_{Rec} /Zn[b](ppm)	$\delta^{66}Zn$[c] (‰)	2SD[d]	$\delta^{68}Zn$[c] (‰)	2SD[d]	N[e]	$\delta^{25}Mg$[c] (‰)	2SDd	$\delta^{26}Mg$[c] (‰)	2SD[d]	N[e]	$\delta^{66}Zn_{Rec}$[f] (‰)	2sd[g]	$\delta^{26}Mg_{Rec}$[f] (‰)	2sd[g]	$\delta^{18}O_{garnet}$[h] (‰)
RV07-31	II	WR		85.3											0.26	0.04	-0.23	0.07	
		garnet	50.0	99.8	0.25	0.01	0.47	0.01	2	-0.29	0.03	-0.56	0.05	6					2.84
		Cpx	50.0	70.9	0.29	0.01	0.62	0.01	2	***0.04***	***0.01***	***0.11***	***0.02***	***3***					
RV07-33	II	WR		74.2											0.29	0.04	-0.25	0.07	
		garnet	50.0	92.5	0.25	0.04	0.52	0.02	2	-0.30	0.01	-0.58	0.03	3					2.58
		Cpx	50.0	55.9	0.35	0.05	0.72	0.04	2	***0.04***	***0.02***	***0.08***	***0.02***	***3***					
RV07-34	II	WR		68.1											0.29	0.04	-0.36	0.07	
		garnet	50.0	72.1	0.28	0.02	0.49	0.04	2	-0.34	0.04	-0.67	0.06	9					2.34
		Cpx	50.0	64.1	0.31	0.03	0.62	0.00	2	***-0.04***	***0.01***	***-0.05***	***0.03***	***3***					
BHVO-2	Basalt				0.32	0.04	0.63	0.08	8										
BIR-1	Basalt				0.2	0.04	0.39	0.07	6	-0.10	0.01	-0.19	0.02	3					
IRMM3702	Pure Zn solution				0.27	0.03	0.55	0.05	38										
AAS	Pure Zn solution				0.04	0.03	0.09	0.05	38										

[a] WR = Whole rock. Garnet and cpx modes are taken from Gréau et al. (2011) and Huang et al. (2012).

[b] Zinc contents of garnet, cpx and reconstructed whole-rock Zn contents (Zn_{Rec}) are taken from Gréau et al. (2011) and Huang et al. (2012) except those marked with bold italics, which were determined and calculated in this study.

[c] $\delta^{X}Zn$ (‰) = $[(^{X}Zn/^{64}Zn)_{sample}/(^{X}Zn/^{64}Zn)_{JMC\ Lyon\ 3702} - 1] \times 1000$, where X = 66 or 68 and JMC Lyon 3072 is an international Zn isotope-normalized standard. $\delta^{X}Mg$ (‰) = $[(^{X}Mg/^{24}Mg)_{sample}/(^{X}Mg/^{24}Mg)_{DSM\text{-}3} - 1] \times 1000$, where X = 25 or 26 and DSM-3 is an international Mg isotope-normalized standard. The Zn-isotope compositions for all samples were determined in this study, while the Mg-isotope compositions were previously reported in Huang et al. (2016a) except for those (marked with bold italics) for garnet from samples RV07-30, -31, -33 and -34, which were determined in this study.

[d] 2SD = two times the standard deviation of the population of N (≥2) repeat measurements of the same solution.

[e] N represents the times of repeated measurements of the same purified solution by MC-ICP-MS.

[f] $\delta^{66}Zn_{Rec}$ (= $\delta^{66}Zn_{Reconstructed}$) and $\delta^{26}Mg_{Rec}$ (= $\delta^{26}Mg_{Reconstructed}$) are the reconstructed whole-rock Zn and Mg isotope compositions of eclogites using modes and element-isotope compositions of garnet and cpx.

[g] 2sd are calculated using error propagation equation $2sd = 2*(SD_1{}^{\wedge 2} + SD_2{}^{\wedge 2})^{\wedge 0.5}$. 2SD are taken as the long-term external reproducibilities of Zn-

(0.03‰) and Mg- (0.05‰) isotope measurements.

[h] Garnet $\delta^{18}O$ values are taken from Huang et al. (2012, 2016a).

[i] Replicate = repeated the whole procedure, including sample dissolution, column chemistry and mass spectrometry.

Table S2. Parameters for calculating the Mg-Zn-O-isotope covariations of mixing MORB and carbonate in Fig. 2a-c.

Comments	δ^{26}Mg (‰)	δ^{18}O (‰)	δ^{66}Zn(‰)	MgO (wt.%)	Zn (ppm)
Calcite	-3	24	0.91	0.8	20
Dolomite	-2	24	0.91	22	132
MORB	-0.25	5.5	0.27	7.5	104

The data of δ^{26}Mg, δ^{66}Zn, MgO and Zn for calcite and dolomite are taken from Liu et al. (2020).
The data of δ^{18}O for calcite and dolomite are taken from Wang et al. (2014).
The data of δ^{26}Mg for MORB are taken from Teng et al. (2010), δ^{18}O for MORB from Cooper et al. (2009), δ^{66}Zn for MORB from Wang et al. (2017) and Huang et al. (2018b), and MgO and Zn for MORB from Jenner and O'Neill. (2012).

Table S3. Modelling parameters for diffusion-induced Zn-Mg-isotope fractionation during melt-peridotite reaction (Fig. 2d).

	$\delta^{66}Zn$	$\delta^{26}Mg$	Zn (ppm)	MgO (wt.%)	D_{Mg}	β_{Mg}	β_{Zn}
Melt	0.27	-0.25	104	7.58	1.98×10^{-6}	0.05	0.06
Perdiotite	0.16	-0.25	53.5	36.7			

Melts have the starting compositions similar to the modern MORB: data for $\delta^{66}Zn$ are taken from Wang et al. (2017) and Huang et al. (2018b), for $\delta^{26}Mg$ from Teng et al. (2010), for Zn from Jenner and O'Neill (2012), for MgO from Hofmann (1988), for D_{Mg} from La Tourrette et al. (1996) and for β_{Mg} from Richter et al. (2009). Emperically derived β_{Zn} for olivine (Huang et al., 2018a) is used here for basaltic melts, because that no β_{Zn} is empirically and experimentally determined for felsic to mafic melts and other minerals. The ratios of D_{Zn}/D_{Mg} are randomly set as 0.5, 1, and 2.

Peridotites have the starting compositions similar to fertile primitive mantle: data for $\delta^{66}Zn$ are taken from Sossi et al. (2018), for $\delta^{26}Mg$ from Teng et al. (2010), for Zn and MgO from Palme and O'Neill (2014).

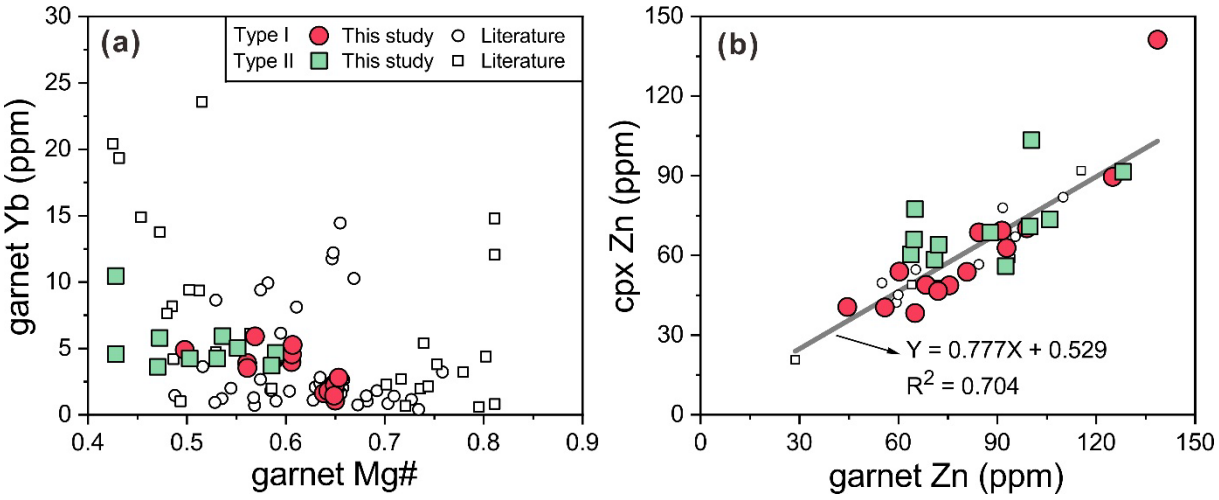

Fig. S1. Yb contents versus Mg# of garnet (a) and Zn contents of garnet and cpx (b) in the Roberts Victor eclogites. The eclogites studied for Zn isotopes are marked with colored symbols, and the other previously-published data were, for comparison, marked with empty symbols. Data are taken from Caporuscio et al. (1990), Schulze et al. (2000), Jacob et al. (2003), Gréau et al. (2011), Huang et al. (2012), Radu et al. (2019) and this study. Dark gray line in (b) is the regression line obtained using the least squares fit.

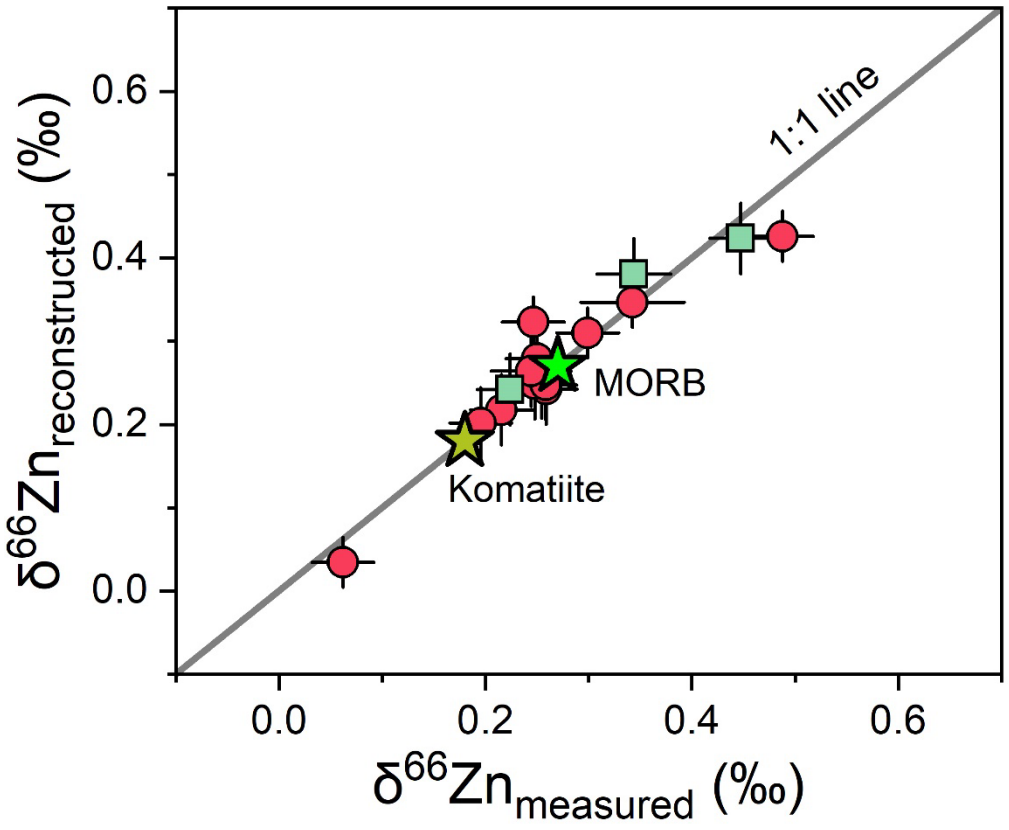

Fig. S2. Comparison of the whole-rock $\delta^{66}Zn$ values measured directly using MC-ICPMS and reconstructed using Zn isotope compositions and modes of garnet and cpx. Dark gray line denote the 1:1 line. Data for MORB are taken from Wang et al. (2017) and Huang et al. (2018b), and for komatiite are taken from Sossi et al. (2018).

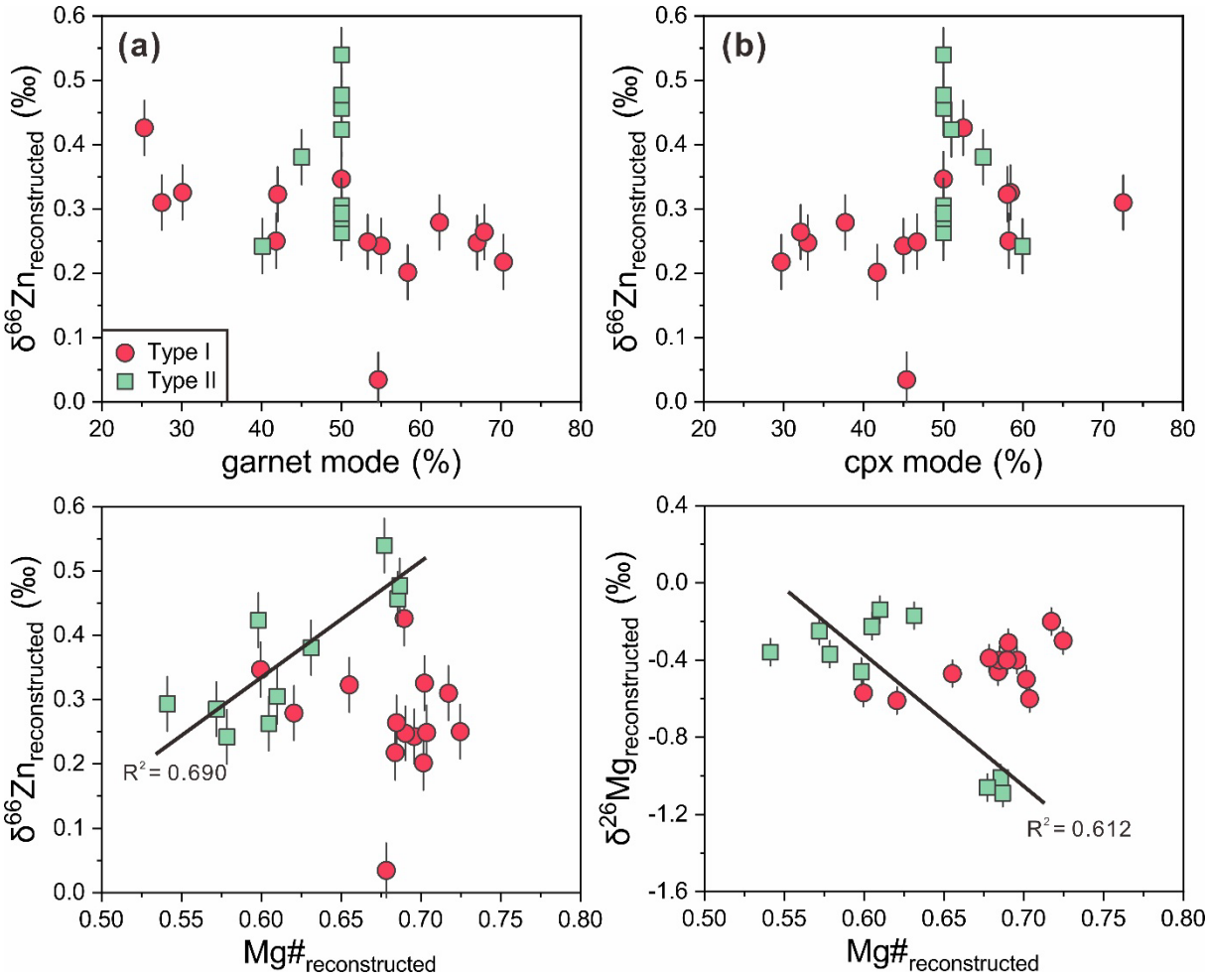

Fig. S3. Reconstructed whole-rock $\delta^{66}Zn$ values versus garnet mode (a), cpx mode (b), and whole-rock Mg# (c), and reconstructed whole-rock $\delta^{26}Mg$ values versus whole-rock Mg# (d) in the Roberts Victor eclogites. Data of mineral modes, whole-rock Mg# and reconstructed whole-rock $\delta^{26}Mg$ values are taken from Gréau et al. (2011) and Huang et al. (2012, 2016a).

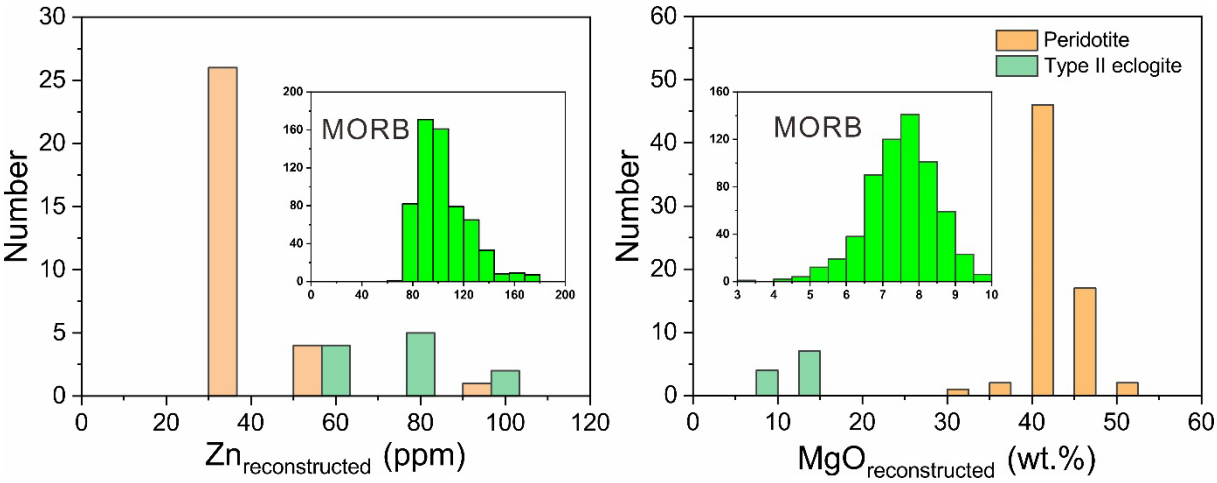

Fig. S4. Compilation of Zn and MgO contents of Type II eclogites from Roberts Victor kimberlites and the surrounding peridotites from the Kaapvaal craton. Data for Type II

eclogites are from Caporuscio et al. (1990), Schulze et al. (2000), Jacob et al. (2003), Gréau et al. (2011), Huang et al. (2012) and Radu et al. (2019). Data for peridotites are from Griffin et al. (2004), Simon et al. (2007), Gibson et al. (2008) and Lazarov et al. (2012). MORB data (inserts) are from Jenner and O'Neill. (2012). The peridotite with high Zn contents had experienced intense metasomatism via fluids/melts (Griffin et al., 2004).

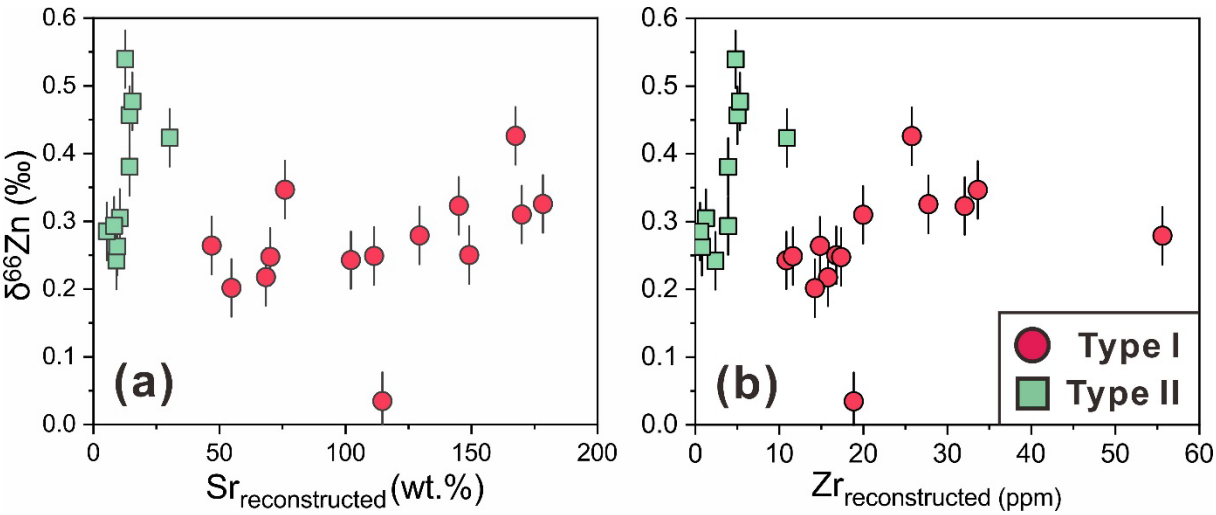

Fig. S5. Reconstructed whole-rock δ^{66}Zn versus Sr (a) and Zr (b) contents of the Roberts Victor eclogites. Element data are taken from Gréau et al. (2011) and Huang et al. (2012).

Supplemental Information References

An Y., Wu F., Xiang Y., Nan X., Yu X., Yang J., Yu H., Xie L., and Huang F., 2014, High-precision Mg isotope analyses of low-Mg rocks by MC-ICP-MS. Chemical Geology, v. 390, p. 9–21. https://doi.org/10.1016/j.chemgeo.2014.09.014.

An, Y., and Huang, F., 2014, A review of Mg isotope analytical methods by MC-ICP-MS: Journal of Earth Science, v. 25, no. 5, p. 822-840, doi. 10.1007/s12583-014-0477-8.

Caporuscio, F. A., and Smyth, J. R., 1990, Trace element crystal chemistry of mantle eclogites: Contributions to Mineralogy and Petrology, v. 105, no. 5, p. 550-561, https://doi.org/10.1007/bf00302494.

Chen, H., Savage, P. S., Teng, F.-Z., Helz, R. T., and Moynier, F., 2013, Zinc isotope fractionation during magmatic differentiation and the isotopic composition of the bulk Earth: Earth and Planetary Science Letters, v. 369–370, no. 0, p. 34-42, http://dx.doi.org/10.1016/j.epsl.2013.02.037.

Chen, S., Liu, Y., Hu, J., Zhang, Z., Hou, Z., Huang, F., and Yu, H., 2016, Zinc isotopic compositions of NIST SRM 683 and whole-rock reference materials. Geostandards and Geoanalytical Research, v. 40(3), p. 417–432, https://doi.org/10.1111/j.1751-908X.2015.00377.x.

Cooper, K. M., Eiler, J. M., Sims, K. W. W., and Langmuir, C. H., 2009, Distribution of recycled crust within the upper mantle: Insights from the oxygen isotope composition of MORB from the Australian-Antarctic Discordance: Geochemistry, Geophysics, Geosystems, v. 10, no. 12, https://doi.org/10.1029/2009GC002728.

Crank J., 1975. The Mathematics of Diffusion. Oxford University Press.

Doucet, L. S., Mattielli, N., Ionov, D. A., Debouge, W., and Golovin, A. V., 2016, Zn isotopic heterogeneity in the mantle: A melting control?: Earth and Planetary Science Letters, v. 451, p. 232-240, http://dx.doi.org/10.1016/j.epsl.2016.06.040.

Hofmann, A. W., 1988, Chemical differentiation of the Earth:the relationship between mantle, continental crust, and oceanic crust: Earth and Planetary Science Letters, v. 90, p. 297-314.

Gréau, Y., Huang, J.-X., Griffin, W. L., Renac, C., Alard, O., and O'Reilly, S. Y., 2011, Type I eclogites from Roberts Victor kimberlites: Products of extensive mantle metasomatism: Geochimica et Cosmochimica Acta, v. 75, no. 22, p. 6927-6954, https://doi.org/10.1016/j.gca.2011.08.035.

Griffin, W. L., Graham, S., O'Reilly, S. Y., and Pearson, N. J., 2004, Lithosphere evolution beneath the Kaapvaal Craton: Re–Os systematics of sulfides in mantle-derived peridotites: Chemical Geology, v. 208, no. 1, p. 89-118, https://doi.org/10.1016/j.chemgeo.2004.04.007.

Huang, J., Chen, S., Zhang, X. C., and Huang, F., 2018a, Effects of Melt Percolation on Zn Isotope Heterogeneity in the Mantle: Constraints From Peridotite Massifs in Ivrea-Verbano Zone, Italian Alps: Journal of Geophysical Research: Solid Earth, v. 123, no. 4, p. 2706-2722, doi:10.1002/2017JB015287.

Huang, J., Liu, S.-A., Gao, Y., Xiao, Y., and Chen, S., 2016b, Copper and zinc isotope systematics of altered oceanic crust at IODP Site 1256 in the eastern equatorial Pacific: Journal of Geophysical Research: Solid Earth, v. 121, no. 10, p. 7086-7100, https://doi.org/10.1002/2016JB013095.

Huang, J., Zhang, X.-C., Chen, S., Tang, L., Wörner, G., Yu, H., and Huang, F., 2018b, Zinc isotopic systematics of Kamchatka-Aleutian arc magmas controlled by mantle melting: Geochimica et Cosmochimica Acta, v. 238, p. 85-101, https://doi.org/10.1016/j.gca.2018.07.012.

Huang, J.-X., Gréau, Y., Griffin, W. L., O'Reilly, S. Y., and Pearson, N. J., 2012, Multi-stage origin of Roberts Victor eclogites: Progressive metasomatism and its isotopic effects: Lithos, v. 142-143, no. Supplement C, p. 161-181, https://doi.org/10.1016/j.lithos.2012.03.002.

Huang, J.-X., Xiang, Y., An, Y., Griffin, W. L., Gréau, Y., Xie, L., Pearson, N. J., Yu, H., and O'Reilly, S. Y., 2016a, Magnesium and oxygen isotopes in Roberts Victor eclogites: Chemical Geology, v. 438, p. 73-83, https://doi.org/10.1016/j.chemgeo.2016.05.030.

Gibson, S. A., Malarkey, J., and Day, J. A., 2008, Melt Depletion and Enrichment beneath the Western Kaapvaal Craton: Evidence from Finsch Peridotite Xenoliths: Journal of Petrology, v. 49, no. 10, p. 1817-1852, https://doi.org/10.1093/petrology/egn048.

Jacob, D. E., Schmickler, B., and Schulze, D. J., 2003, Trace element geochemistry of coesite-bearing eclogites from the Roberts Victor kimberlite, Kaapvaal craton: Lithos, v. 71, no. 2, p. 337-351, https://doi.org/10.1016/S0024-4937(03)00120-8.

Jenner, F. E., and O'Neill, H. S. C., 2012, Analysis of 60 elements in 616 ocean floor basaltic glasses: Geochemistry, Geophysics, Geosystems, v. 13, no. 2, p. n/a-n/a, https://doi.org. 10.1029/2011GC004009.

LaTourrette, T., Wasserburg, G. J., and Fahey, A. J., 1996, Self diffusion of Mg, Ca, Ba, Nd, Yb, Ti, Zr, and U in haplobasaltic melt: Geochimica et Cosmochimica Acta, v. 60, no. 8, p. 1329-1340, https://doi.org/10.1016/0016-7037(96)00015-4.

Lazarov, M., Brey, G. P., and Weyer, S., 2012, Evolution of the South African mantle—a case study of garnet peridotites from the Finsch diamond mine (Kaapvaal craton); Part 2: Multiple depletion and re-enrichment processes: Lithos, v. 154, p. 210-223, https://doi.org/10.1016/j.lithos.2012.07.013.

Liu, S.-A., Wang, Z.-Z., Yang, C., Li, S.-G., and Ke, S., 2020, Mg and Zn Isotope Evidence for Two Types of Mantle Metasomatism and Deep Recycling of Magnesium Carbonates: Journal of Geophysical Research: Solid Earth, v. 125, no. 11, p. e2020JB020684, doi. https://doi.org/10.1029/2020JB020684.

Liu, Y., Hu, Z., Gao, S., Günther, D., Xu, J., Gao, C., and Chen, H., 2008, In situ analysis of major and trace elements of anhydrous minerals by LA-ICP-MS without applying an internal standard: Chemical Geology, v. 257, no. 1, p. 34-43, https://doi.org/10.1016/j.chemgeo.2008.08.004.

Moynier, F., Vance, D., Fujii, T., and Savage, P., 2017, The Isotope Geochemistry of Zinc and Copper: Reviews in Mineralogy and Geochemistry, v. 82, no. 1, p. 543-600, https://dor.org.10.2138/rmg.2017.82.13.

Palme, H., and O'Neill, H. S. C., 2014, 3.1 - Cosmochemical Estimates of Mantle Composition, *in* Holland, H. D., and Turekian, K. K., eds., Treatise on Geochemistry (Second Edition): Oxford, Elsevier, p. 1-39.

Radu, I.-B., Harris, C., Moine, B. N., Costin, G., and Cottin, J.-Y., 2019, Subduction relics in the subcontinental lithospheric mantle evidence from variation in the δ18O value of eclogite xenoliths from the Kaapvaal craton: Contributions to Mineralogy and Petrology, v. 174, no. 3, p. 19, https://doi.org/10.1007/s00410-019-1552-z.

Richter, F. M., Dauphas, N., and Teng, F.-Z., 2009, Non-traditional fractionation of non-

traditional isotopes: Evaporation, chemical diffusion and Soret diffusion: Chemical Geology, v. 258, no. 1, p. 92-103, https://doi.org/10.1016/j.chemgeo.2008.06.011.

Schulze, D. J., Valley, J. W., and Spicuzza, M. J., 2000, Coesite eclogites from the Roberts Victor kimberlite, South Africa: Lithos, v. 54, no. 1, p. 23-32, https://doi.org/10.1016/S0024-4937(00)00031-1.

Simon, N. S. C., Carlson, R. W., Pearson, D. G., and Davies, G. R., 2007, The Origin and Evolution of the Kaapvaal Cratonic Lithospheric Mantle: Journal of Petrology, v. 48, no. 3, p. 589-625, https://doi.org.10.1093/petrology/egl074.

Sossi, P. A., Halverson, G. P., Nebel, O., and Eggins, S. M., 2015, Combined Separation of Cu, Fe and Zn from Rock Matrices and Improved Analytical Protocols for Stable Isotope Determination: Geostandards and Geoanalytical Research, v. 39, no. 2, p. 129-149, https://doi.org.10.1111/j.1751-908X.2014.00298.x.

Teng, F.-Z., 2017, Magnesium Isotope Geochemistry. Reviews in Mineralogy and Geochemistry, v. 82, p. 219–287. https://doi.org/10.2138/rmg.2017.82.7.

Yang, Y., Zhang, X., Liu, S.-A., Zhou, T., Fan, H., Yu, H., et al. (2018). Calibrating NIST SRM 683 as a new international reference standard for Zn isotopes. Journal of analytical Atomic Spectrometry, v. 33(10), p. 1777–1783.doi. https://doi.org/10.1039/C8JA00249E.

Teng, F.-Z., Li, W.-Y., Ke, S., Marty, B., Dauphas, N., Huang, S., Wu, F.-Y., and Pourmand, A., 2010, Magnesium isotopic composition of the Earth and chondrites: Geochimica et Cosmochimica Acta, v. 74, no. 14, p. 4150-4166, doi.10.1016/j.gca.2010.04.019.

Wang, S.-J., Teng, F.-Z., and Li, S.-G., 2014, Tracing carbonate–silicate interaction during subduction using magnesium and oxygen isotopes: Nat Communications, v. 5, doi. 10.1038/ncomms6328.

Wang, Z.-Z., Liu, S.-A., Liu, J., Huang, J., Xiao, Y., Chu, Z.-Y., Zhao, X.-M., and Tang, L., 2017, Zinc isotope fractionation during mantle melting and constraints on the Zn isotope composition of Earth's upper mantle: Geochimica et Cosmochimica Acta, v. 198, p. 151-167, http://dx.doi.org/10.1016/j.gca.2016.11.014.